

# Clutter suppression and classification using twin inverted pulse sonar in ship wakes

T. G. Leighton,<sup>a)</sup> D. C. Finfer, G. H. Chua, and P. R. White

*Institute of Sound and Vibration Research, University of Southampton, Highfield, Southampton SO17 1BJ, UK*

J. K. Dix

*School of Ocean and Earth Sciences, National Oceanography Centre, Southampton, European Way, Southampton SO14 3ZH, UK*

(Received 13 October 2010; revised 26 February 2011; accepted 2 March 2011)

Twin inverted pulse sonar (TWIPS) is here deployed in the wake of a moored rigid inflatable boat (RIB) with propeller turning, and then in the wake of a moving tanker of 4580 dry weight tonnage (the *Whitchallenger*). This is done first to test its ability to distinguish between scatter from the wake and scatter from the seabed, and second to test its ability to improve detectability of the seabed through the wake, compared to conventional sonar processing techniques. TWIPS does this by distinguishing between linear and nonlinear scatterers and has the further property of distinguishing those nonlinear targets which scatter energy at the even-powered harmonics from those which scatter in the odd-powered harmonics. TWIPS can also, in some manifestations, require no range correction (and therefore does not require the *a priori* environment knowledge necessary for most remote detection technologies).

© 2011 Acoustical Society of America. [DOI: 10.1121/1.3626131]

PACS number(s): 43.30.Vh, 43.25.Yw, 43.30.Lz [EJS]

Pages: 3431–3437

## I. INTRODUCTION

Twin inverted pulse sonar (TWIPS) is a process by which a source emits a pressure time series,  $p(t) = \Gamma(t) - \Gamma(t - \Delta)$ , which consists of a pulse  $\Gamma(t)$  followed, an inter-pulse time  $\Delta$  later, by a pulse which is identical except that it has opposite polarity to the first pulse.<sup>1</sup> Consider a scenario where the environment is noise-free,  $\Delta$  is sufficiently long that there is no overlap between the outgoing pulses, and no second harmonic distortion is introduced to the outgoing pulse by, say, the power amplifier. Then construct the signal  $p_+(t)$  by adding together the echoes from scatterers, where the first echo has been delayed by  $\Delta$ . In such conditions, if the environment contains linear scatterers which have not evolved between the two pulses,  $p_+(t)$  should equal 0 (since if the scattering dynamics are linear, the principle of superposition will hold even with the ring-up and ringdown that are characteristic of bubbles<sup>2</sup>). Non-zero components from a field of only linear scatterers would indicate evolution, which could for example be used to detect the disturbance of soil between the two pulses and be used for sonar or radar detection of such<sup>1</sup> as will be explained. If there are nonlinear scatterers, these will also give non-zero components in the summation. This has been used for the detection of ultrasonic contrast agents<sup>3</sup> (although there the narrow size distribution of bubbles present allows easy excitation of nonlinearity through single bubble resonance,<sup>4,5</sup> which is not so simple a task in the ocean where the bubble size distribution spans many decades in radius<sup>6</sup>). If instead the second echo is subtracted from the delayed version of the first echo,

to form  $p_-(t)$ , then the even-powered harmonic components of any nonlinear scatter become 0. Non-zero returns indicate scattering from linear scatterers, and scattering of the fundamental and odd-powered harmonics from nonlinear scatterers.<sup>7,8</sup> This allows further discrimination between linear scatterers, nonlinear scatterers that scatter in odd harmonics, and those which scatter in even harmonics. This potential richness of harmonic detection might have uses outside sonar: TWIPR (twin inverted pulse radar) might be used to distinguish between soil (which scatters linearly), rusty metal (which predominantly scatter odd harmonics), and semiconductors (which scatter all harmonics), with application to the detection of improvised explosive devices and in-wall surveillance equipment.<sup>1</sup> Since  $p_-(t)$  contains energy from both linear and nonlinear scatterers, ratios based on  $p_-(t)$  and  $p_+(t)$  can be used to enhance the linear with respect to the nonlinear scatterers in an image field. Such ratios have the additional useful property that they do not require range correction, for example, through the use of time varying gain.<sup>1</sup> This obviates the need for *a priori* knowledge of propagation losses that would be required if range correction were undertaken. Such *a priori* knowledge would be difficult to obtain in wakes or the surf zone<sup>9</sup> where, at a given point in the water column, the sound speed and attenuation can vary significantly on time-scales less than 1 s.

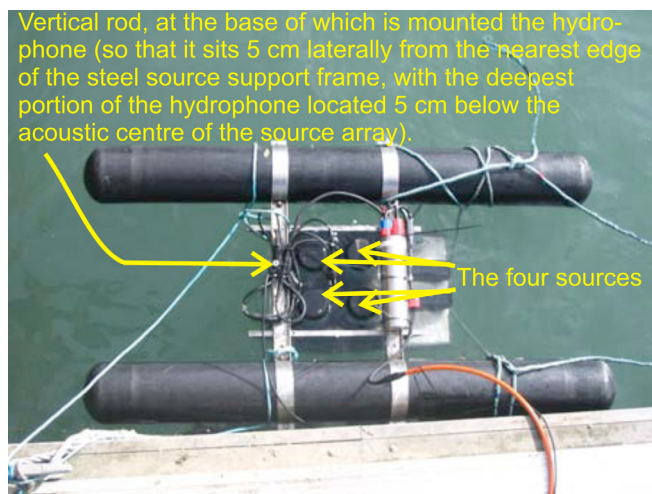
The TWIPS system has been described in detail elsewhere,<sup>1</sup> although with just one sea trial result. The purpose of this paper is to provide further sea trial data (raw and processed data for this study are available for download<sup>10</sup>). In this study, a TWIPS system is deployed near the sea surface in the wake of a moored rigid inflatable boat (RIB) with its propeller turning, and then it is towed in the wake of a tanker of 4580 dry weight tonnage. This is done first to test

<sup>a)</sup>Author to whom correspondence should be addressed. Electronic mail: [tgl@soton.ac.uk](mailto:tgl@soton.ac.uk)

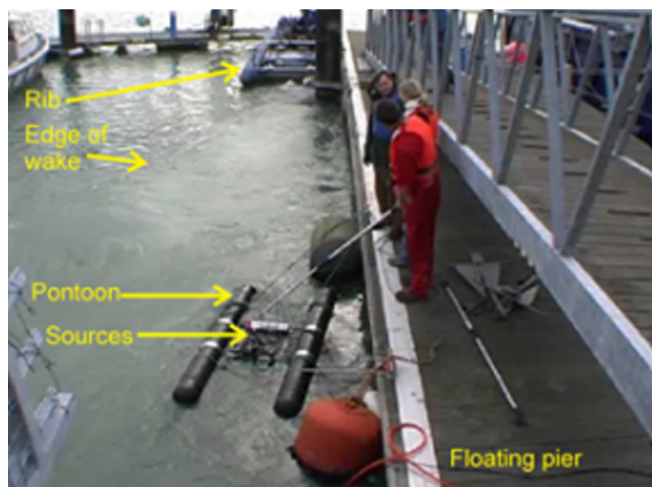
its ability to distinguish between scatter from the wake and scatter from the seabed, and second to test its ability to improve detectability of the seabed through the wake.

## II. METHOD

Two sea trials were conducted, both using a sonar source made from four acoustic transmitters (GeoAcoustics T135D transducers) arranged in a  $2 \times 2$  configuration. For the *Whitchallenger* tests the source was towed as described for the sea trials in Ref. 1, whilst for the RIB tests the source were mounted on a pontoon [Fig. 1(a)]. The directivity of this source, and the time histories of the 8-cycle 6 kHz pulses (with Gaussian envelopes) emitted by this source, are plotted by Leighton *et al.*<sup>1</sup> The presence of side lobes must be borne in mind when interpreting sonar images, especially as the



A



B

FIG. 1. (Color online) (a) The dockside sea trial (26 February 2008). This photo shows a downward looking view of the pontoon supporting the four sources in a  $2 \times 2$  array. When the system is lowered into the water, the acoustic center of the array is located approximately 20 cm below the surface. (b) The 26 February 2008 test where the downward looking TWIPS sources are mounted in a pontoon and placed in the wake of a moored RIB. See Ref. 36 for a movie of this trial taking place. The movie can also be found at the web page given in Ref. 10 associated with this article.

arrangements for both sea trials were practical rather than idealized and optimized, so that there were numerous reflecting structures (piers, ship sterns, air/sea interfaces, etc.) that could give to spurious reflections from a side lobe that the sonar imaging would interpret as on-axis scatter. Although TWIPS should work with a range of pulse types (chirp, pseudorandom), in this experiment only the pulse amplitude and interpulse delay were within the control of the operator, and the pulses used must satisfy some basic criteria. The amplitude at target must be sufficiently great to excite a nonlinearity if that is required (although not all TWIPS applications require this, as the soil disturbance example of Sec. I shows). The simple results described in Sec. I (that obtain zeros for certain components when adding and subtracting the two echoes), rely on the delay  $\Delta$  being large enough such that the response to  $\Gamma(t)$  has decayed sufficiently so as to be negligible prior to the start of  $\Gamma(t - \Delta)$ . This imposes a lower limit on the selection of  $\Delta$ , such that one has to use an inter-pulse delay large enough so that all echoes from the first pulse have decayed before the second pulse is emitted. A delay of  $\Delta = 50$  ms was suitable for these trials, which can also be seen as setting a maximum range over which a TWIPS based system can operate; the maximum range being given by  $c_0\Delta/2$  (which corresponds roughly to 37.5 m for the 50 ms inter-pulse delay used here). For the application under consideration here, when evolution of the scattering environment degrades performance (unlike the soil disturbance example in Sec. I where evolution is key to performance), there is also a maximum value of  $\Delta$  which can be tolerated. The performance of TWIPS in the application studied here reduces by  $\sim 50\%$  when relative motion between the scatterers and platform generates the path length differences corresponded to  $0.37\lambda$ , where  $\lambda$  is the acoustic wavelength. In the open water tests, where the source is towed at 4 knots ( $\sim 2$  m  $s^{-1}$ ), assuming a sound speed of no more than 1500 m  $s^{-1}$  in the (admittedly bubbly) seawater,  $0.37\lambda$  corresponds to no more than  $\sim 10$  cm if only one receiver is available (as here), which means that an interpulse time of 50 ms provides a useful compromise between the two limiting factors on  $\Delta$ .

The sonar images in this paper plot smoothed envelopes of the basic signals  $p(t)$ ,  $p_+(t)$  and  $p_-(t)$  which are computed by band-pass filtering the signals, then computing their envelope (exploiting the Hilbert transform) and finally smoothing the result by averaging over the duration of the outgoing pulse. These smoothed envelopes are denoted here using capital  $P$  notation, so that the envelopes of  $p(t)$ ,  $p_+(t)$  and  $p_-(t)$  are denoted  $P$ ,  $P_{2+}$  and  $P_{1-}$ , respectively (the subscripts “1” and “2” indicating the application of bandpass filters centered about the first and second harmonics, respectively, in the initial stage of this processing).

The same echoes are processed three ways, so that the performance of  $P_{1-}/P_{2+}$  (which should suppress the wake) can be compared with that of  $P_{2+}$  (which should highlight the bubbles). Both are compared with “conventional” sonar processing. In this, the returned signal is band-pass filtered about the center frequency of the outgoing pulse, and then the energy of the return is computed by temporally averaging the envelope using a period which corresponds to the

duration of the original pulse, and the final output calculated from the average of the results from both TWIPS pulses so that this “conventional” technique is not inherently disadvantaged relative to TWIPS.

While the ratio  $P_{1-}/P_{2+}$  obviates the need for time varying gain, this comes with the disadvantage of instability.<sup>1,11</sup> Here, fluctuations in the denominator are reduced through geometrical averaging of values of  $P_{2+}$  over sets of adjacent returns. For each image plot shown, a noise level thresholding is also performed to eliminate spurious variation due to very low echo returns and noise. The noise level thresholding is implemented by neglecting samples whose value is less than 1% of the maximum value in the plot.

Note that the hydrophone is placed in front of the acoustic sources [Fig. 1(a)]. Given that inducement of a bubble nonlinearity requires high amplitude pulses, data on the outgoing pulse (excluded from the processing here) in such arrangements are liable to clipping. It is interesting to note that TWIPS has the useful property of detecting clipped data. Symmetrical clipping of the peak positive and peak negative parts of a signal introduces odd harmonic components as artifacts which were not present in the original signal, and these would be emphasized in  $P_-$  and suppressed in  $P_+$ . In many practical situations, where clipping occurs it is asymmetrical and, therefore, its influence on  $P_-$  and  $P_+$  is more complicated.

The objective of both sea trials was to detect the seabed through a wake. Assessment of effectiveness is through visibility of the seabed in the sonar images. While performance could not be quantified through Receiver Operator Characteristics curves since the measurements cannot be redone with the seabed removed,<sup>1</sup> nevertheless the wake clutter reduction ratio can be calculated as  $10 \log_{10}(E_{TWIPS}/E_{STAND})$  where  $E_{TWIPS}$  (the “energy” associated with the TWIPS function in question) is first computed by summing the TWIPS values over a region where there is wake, and where  $E_{STAND}$  is the energy associated with the conventional or standard sonar processing over the same location. To prevent simple gains in the system from affecting the measure,  $E_{TWIPS}$  and  $E_{STAND}$  are both normalized with the respective average value of the echo returns from the sea floor (which is the target here).

The first sea trial, on 26 February 2008, used a moored RIB to generate the wake. While use of multiple hydrophones would have provided ready distinction between outward and returning pulses, only one hydrophone was available (Blacknor Technology D140, serial number 18938 with built-in preamplifier, calibrated by the National Physical Laboratory). It was mounted with the downward looking acoustic sources in a pontoon located 7.8 m downstream from the RIB, in its wake [Fig. 1(b)]. The RIB and pontoon were moored to the dockside at the National Oceanography Centre, Southampton. For the second sea trial, on 27 February 2008, the same configuration of sources and sensors was mounted in a towfish and towed 2–4 m behind the stern of the *RV Bill Conway* at ~1.5 m depth through the wakes of various vessels<sup>12</sup> as the *RV Bill Conway* sailed from the National Oceanography Centre (Southampton) (50°53'33"N, 1°23'38"W) to Calshot Castle (50°49'11.53"N, 1°18'23.17"W). Representative results are presented for the tanker

*Whitchallenger*. The trials took place in the very busy shipping lanes of Southampton Water (which handles 7% of the UK's entire seaborne trade), where the seabed varies between 10 and 20 m depth. A time varying gain [proportional to  $r^2(t)$  where  $r(t)$  is the penetration depth at time  $t$ ] was applied to all the echoes before processing to allow fair comparison between the conventional sonar and TWIPS results (noting that any such correction cancels out in the TWIPS function  $P_-/P_+$ ).

The experimental results are compared to simulations undertaken using the method described by Leighton *et al.*<sup>1</sup> Two types of wake are studied in the simulations, one reflecting the wake of a “small” vessel and another reflecting the wake of a “large” vessel. Although equipment was prepared to measure the bubble size distributions (BSDs) in the wakes,<sup>13</sup> budget limitations prevented its deployment. The published literature contains few such measurements, and so therefore best estimates (Fig. 2) had to be made to provide BSDs as input for the simulations.

Although wakes have for decades been known to scatter sound and strongly influence sound speed<sup>14</sup> and attenuation,<sup>15–17</sup> there are few measurements which would enable one to produce maps of the BSD as the wake is shaped and evolves behind the ship through buoyancy and flow<sup>18,19</sup> etc. In wakes, the BSD is expected to vary in time<sup>20</sup> and depend on the ship speed and characteristics, the age of the wake and the water quality.<sup>21</sup> However, there is only limited information on how the map of BSD in the wake varies with the ocean environment and with ship operating conditions, such as vessel speed and trim.<sup>22</sup> Some studies measured the BSD by fixing a sensor into position,<sup>23,24</sup> and then monitoring the wake as a vessel steers close to the sensor. In this way, as time progresses the data refers to the aging process of one element of the wake. Alternatively, a sensor can be towed

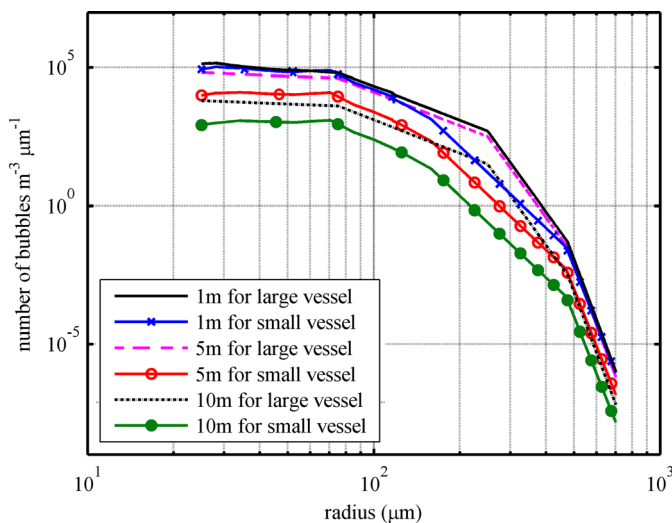


FIG. 2. (Color online) Bubble size distributions (BSDs) used in the simulations at several depths (indicating the number of bubbles per cubic meter of bubbly water, per micron increment in bubble radius). The lines show the following BSDs: at a depth of 1 m for a large vessel (solid line) and a small vessel (solid line with cross markers), at a depth of 5 m for the large vessel (dashed line) and the small vessel (solid line with open circle markers), and at a depth of 10 m for the large vessel (dotted line) and the small vessel (solid line with closed circle markers).

through or beside the wake<sup>25,26</sup> or mounted on an AUV,<sup>27,28</sup> such that the sensor moves through the water with the wake or relative to it which can in principle allow mapping of the bubble population in different parts of the wake.<sup>29</sup>

To provide input for the simulations involving the RIB, a representative wake for a “small” vessel was constructed from the data in Event B of Valge and Burch.<sup>30</sup> To compare with the *Whitchallenger* data, a representative “large” vessel wake was based on the data of Culver and Trujillo.<sup>31</sup> Because the wake at a given point depends on its age and the vessel speed, and because no match to the *Whitchallenger* measurement conditions was found in the literature, several assumptions were applied to generate a “large” vessel distribution that might be compared to the *Whitchallenger* measurement conditions. First, the bubble size distribution for radii outside that presented by Culver and Trujillo is extrapolated from the “small” vessel wake data in the absence of data on such bubble sizes for similar vessels. Second, the factor of 2 is used to compensate for the fact that *Whitchallenger* was, at 5 knots, traveling more slowly than the 16 knots vessel measured by Culver and Trujillo. To scale their results to the current case, the algorithm incorporates the finding that the fraction of air present as bubbles in a measured destroyer wake decreased from  $2.3 \times 10^{-7}$  to  $1.4 \times 10^{-7}$  per cubic centimeter when the ship speed decreased from 20 to 10 knots for a wake age of 3 min.<sup>32</sup> Hence, a factor of 2 (rounded to the nearest whole number) is used. The wake profile has been simplified by assuming that, below a critical depth, the wake density decays with increasing depth, but the density is constant above a critical depth. Measurements support this approximate model.<sup>23</sup> The critical depth was set based on the estimated depth of the propeller axis of each vessel. For the RIB, this was estimated to be 0.5 m. For the *Whitchallenger*, this was estimated to be 4 m. The fully laden draft of *Whitchallenger* is approximately 6 m. At time of measurement, the vessel was also observed to be not fully laden. Below this depth, the wake density is assumed for both vessels to decrease exponentially with depth, with an e-folding scale of 1.5 m, consistent with Farmer and Lemon.<sup>33</sup>

### III. RESULTS AND DISCUSSION

Pairs of pulses are emitted once per second from the downward looking sonar to examine the seabed through the wake. Each consecutive pair of echoes is processed (a) in the “conventional” manner, (b) to calculate  $P_{1-}/P_{2+}$ , and (c) to calculate  $P_{2+}$ . The resulting echo lines are therefore generated once per second, and hence when stacked they form an image (with amplitude represented by color, as defined in the color bar). In the moored tests of Fig. 3(a), conventional sonar shows the wake and there are occasional very faint returns from the seabed. TWIPS increases the detectability of the seabed in Fig. 3(b) and furthermore provides discrimination between seabed and wake, since the seabed is visible when using  $P_{1-}/P_{2+}$  in Fig. 3(b) and not when using  $P_{2+}$  in Fig. 3(c), while the opposite is true of the wake. Sidelobe scatter from pontoon struts is also linear, and so is enhanced

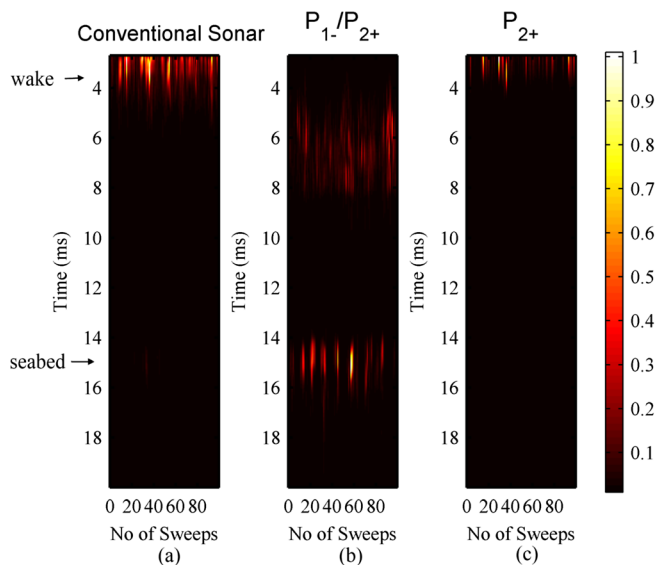


FIG. 3. (Color online) Comparison of three processing types for the same set of raw data (taken in the moored tests of Fig. 1 with an interpulse time of 50 ms and presented using a linear color scale normalized to its maximum value shown in { } brackets): (a) Conventional sonar {max =  $5.1 \times 10^2$ }; (b)  $P_{1-}/P_{2+}$  {max =  $2.4 \times 10^6$ }; and (c)  $P_{2+}$  {max = 5.8}. For all three representations, noise level thresholding was set at 1% of maximum value and geometric averaging was carried out for each ten lines in the denominator of (b).

(at 6–8 ms) in Fig. 3(b) but suppressed in Fig. 3(c). The wake clutter reduction ratios<sup>1</sup>  $10 \log_{10}(E_{\text{TWIPS}}/E_{\text{STAND}})$  in this moored test was  $-26.3$  dB for  $P_{1-}/P_{2+}$  and  $-54.7$  dB for  $P_{1-}/P_{2+}^2$  (image not shown). The results of the “small” vessel simulations (Fig. 4) show similar trends, although exact agreement is not expected given the estimates required

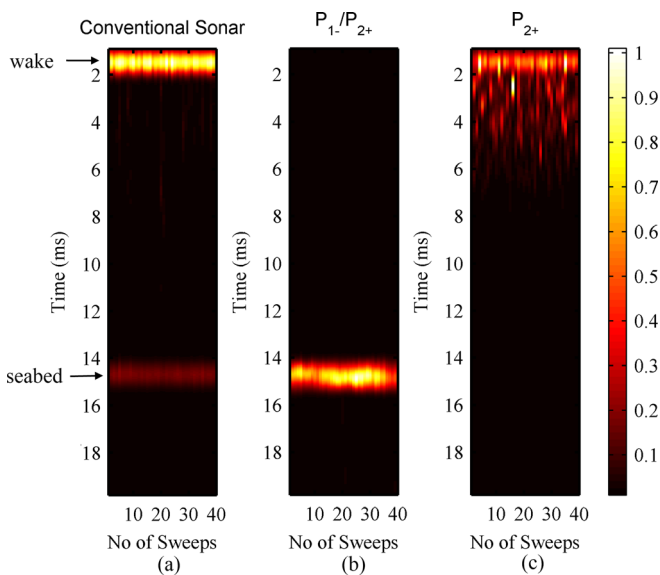


FIG. 4. (Color online) Comparison of three processing types for a set of simulated data (based on wake of a small vessel) and presented using a linear color scale normalized to its maximum value shown in { } brackets): (a) Conventional sonar {max =  $1.4 \times 10^{12}$ }; (b)  $P_{1-}/P_{2+}$  {max =  $8.9 \times 10^4$ }; and (c)  $P_{2+}$  {max =  $1.3 \times 10^{12}$ }. For all three representations, noise level thresholding was set at 1% of maximum value and geometric averaging was carried out for each ten lines in the denominator of (b).

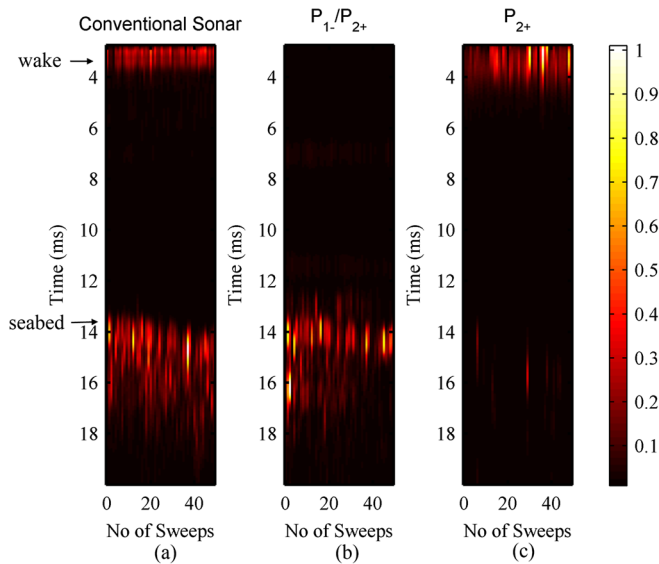


FIG. 5. (Color online) Data taken with the TWIPS source in the wake of the *RV Bill Conway* only. Comparison of three processing types for the same set of raw data (taken with an interpulse time of 50 ms and presented using linear color scale having a maximum value shown in {} brackets): (a) Conventional sonar {max =  $5.6 \times 10^2$ }; (b)  $P_{1-}/P_{2+}$  {max =  $9.2 \times 10^5$ }; and (c)  $P_{2+}$  {max = 1.1}. For all three representations, noise level thresholding was set at 1% of maximum value and geometric averaging was carried out for each ten lines in the denominator of (b).

of the input for the bubble and seabed and different setup conditions [and of course the maximum values in captions for (a) and (c) will differ significantly between simulations (based on pressure) and measurements (based on voltage including amplifier gain); and the denominator in (b) will be sensitive to absorption and noise]. For example, the seabed echo in Fig. 4(a) is stronger than that in Fig. 3(a), probably



FIG. 6. (Color online) Approaching the wake of the tanker *Whitchallenger* (measuring 85 m  $\times$  15 m, with 2965 gt, 4580 dwt) just prior to taking sonar records of Fig. 7. Data is not shown for *RV Bill Conway's* commercial depth sounder (Wheel house unit: Simrad CR50 with Transducer: Simrad combi C50/200 dual 50 kHz/200 kHz operating at 200 kHz) which was not operable in the wake of the vessel. See Ref. 36 for a movie of the entry into the wake of *Whitchallenger*. The movie can also be found at the web page given in Ref. 10 associated with this article.

because the setup in Fig. 4 was for a moving boat since that is the scenario from which the bubble size distribution data were obtained. In contrast, for Fig. 3 the boat was moored with the wake projected toward a quay [Fig. 1(b) was taken from the quay]. Since the sonar was only meters from the quay [Fig. 1(b)], the wake was partially confined and its density likely to be greater than that measured for the moving boat, giving greater attenuation. Note also in comparing field data (Fig. 3) with simulations (Fig. 4) that the first few milliseconds of field data cannot be shown because of overlap with the time during which the source is transmitting.

The following day, the source was towed. Prior to entering the wakes of a second vessel, the performance of TWIPS as it was towed behind the *RV Bill Conway* at 4 knots was tested. This gives an indication of the effect of the wake of the *RV Bill Conway* alone. The results (Fig. 5) in this instance do not show dramatic improvement afforded by TWIPS in the detectability of the seabed by the source: the target (seabed) is sufficiently strong to be detectable without TWIPS, given the 1.5 m towing depth of the sensor. However, comparison of Figs. 5(b) and 5(c) enables classification of the scatterers, indicating which are bubbles and which are sediment. The wake clutter reduction ratios  $10 \log_{10}(E_{TWIPS}/E_{STAND})$  in Fig. 5 are  $-18.1$  dB for the TWIPS function  $P_{1-}/P_{2+}$ , and  $-50.5$  dB for the TWIPS function  $P_{1-}/P_{2+}^2$  (image not shown).

The *RV Bill Conway* then entered at 4 knots the wake of the large vessel *Whitchallenger* (Fig. 6) (results for the wake of the *MV Red Osprey* were shown earlier<sup>1</sup>). In the wake of *Whitchallenger*, conventional sonar processing identifies the wake but scatter from the seabed is barely discernable [Fig. 7(a)]. TWIPS ( $P_{1-}/P_{2+}$ ) in contrast scatters strongly from the seabed and wake scatter is

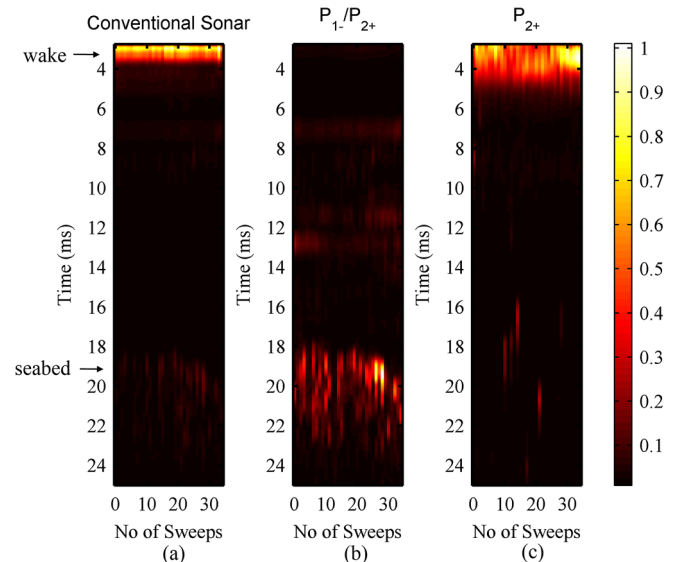


FIG. 7. (Color online) Data taken in the wake of the *Whitchallenger* (Fig. 6). Comparison of three processing types for the same set of raw data (taken with an interpulse time of 50 ms and presented using linear color scale having a maximum value shown in {} brackets): (a) Conventional sonar {max =  $1.9 \times 10^2$ }; (b)  $P_{1-}/P_{2+}$  {max =  $1.2 \times 10^5$ }; and (c)  $P_{2+}$  {max =  $2.7 \times 10^{-1}$ }. For all three representations, noise level thresholding was set at 1% of maximum value and geometric averaging was carried out for each ten lines in the denominator of (b).

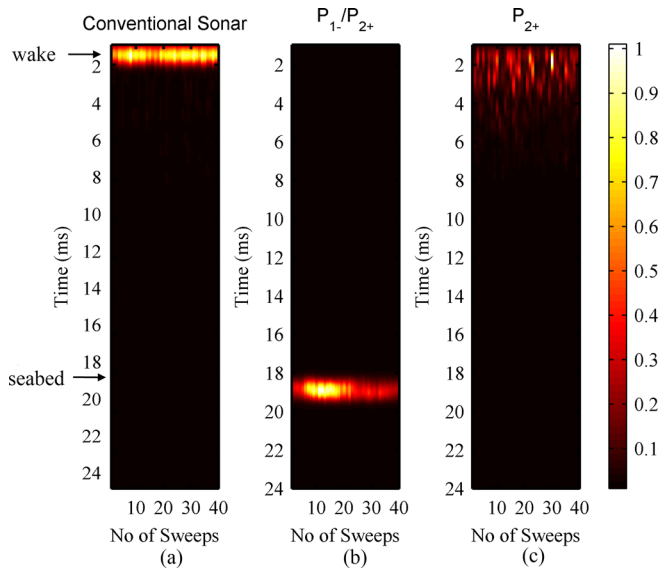


FIG. 8. (Color online) Comparison of three processing types for a set of simulated data (based on wake of a large vessel and presented using a linear color scale normalized to its maximum value shown in {} brackets): (a) Conventional sonar { $\max = 6.3 \times 10^{12}$ }; (b)  $P_{1-}/P_{2+}$  { $\max = 4.4 \times 10^4$ }; and (c)  $P_{2+}$  { $\max = 2.8 \times 10^{13}$ }. For all three representations, noise level thresholding was set at 1% of maximum value and geometric averaging was carried out for each ten lines in the denominator of (b).

suppressed [Fig. 7(b)], while in Fig. 7(c)  $P_{2+}$  scatters strongly from the wake.

Similar observations can be made when these circumstances are simulated using the “large” vessel model (Fig. 8). This was carried out for a seabed at about 19 ms and an ideally stable platform.

#### IV. CONCLUSIONS

A downward looking TWIPS source was tested in the wake of a moored RIB, and when towed in the wake of the *RV Bill Conway* both with and without the additional wake of another vessel (*Whitchallenger*, the results for *MV Red Osprey* having been shown earlier<sup>1</sup>). Use of  $P_{-}/P_{+}$  generally improved the detectability of the seabed, which usually provided only a faint echo with conventional sonar processing. Furthermore, comparison of the TWIPS  $P_{-}/P_{+}$  and  $P_{+}$  functions always enabled discrimination of the returns from the wake and the seabed (conventional sonar inherently has no capability for discrimination, which is why bubble-based torpedo countermeasures were proposed). At-sea discrimination between bubbles and linear scatterers has potential military applications in mine countermeasures and target counter-countermeasures, and for the detection of gas in marine sediment<sup>34</sup> or pipelines.<sup>35</sup> Even in the absence of nonlinear scatterers, applications for monitoring for sediment disturbance have been outlined, which could be extrapolated to land-based sediments using radar. Furthermore on land, nonlinear scattering of both acoustic and electromagnetic waves from buried mines could be exploited using these methods.

#### ACKNOWLEDGMENTS

This work received no external funding (support was provided via T.G.L.’s consultancy activity and a contribution

to Dan Finfer’s studentship by ISVR). Since these funds could not cover the cost of this project, the authors wish to thank a number of people for free donation of time and facilities: students Dave Coles and Anne-Marie Liszczyk, the Skipper (Bob Wilkie) and crew (John Davies) of the *RV Bill Conway*, and Kevin Padley (boat skipper of the RIB). Professor Peter Thorne provided very useful comments as Dan Finfer’s external Ph.D. examiner.

- <sup>1</sup>T. G. Leighton, D. C. Finfer, P. R. White, G.-H. Chua, and J. K. Dix, “Clutter suppression and classification using Twin Inverted Pulse Sonar (TWIPS),” *Proc. R. Soc. A* **466**, 3453–3478 (2010).
- <sup>2</sup>J. W. L. Clarke and T. G. Leighton, “A method for estimating time-dependent acoustic cross-sections of bubbles and bubble clouds prior to the steady state,” *J. Acoust. Soc. Am.* **107**(4), 1922–1929 (2000).
- <sup>3</sup>D. H. Simpson, C. T. Chin, and P. N. Burns, “Pulse inversion Doppler: A new method for detecting nonlinear echoes from microbubble contrast agents,” *IEEE Trans. Ultrasonics, Ferroelectrics Frequency Control* **46**(2), 372–382 (1999).
- <sup>4</sup>T. G. Leighton, A. D. Phelps, D. G. Ramble, and D. A. Sharpe, “Comparison of the abilities of eight acoustic techniques to detect and size a single bubble,” *Ultrasonics* **34**, 661–667 (1996).
- <sup>5</sup>T. G. Leighton, D. G. Ramble, and A. D. Phelps, “The detection of tethered and rising bubbles using multiple acoustic techniques,” *J. Acoust. Soc. Am.* **101**(5), 2626–2635 (1997).
- <sup>6</sup>A. D. Phelps and T. G. Leighton, “Oceanic bubble population measurements using a buoy-deployed combination frequency technique,” *IEEE J. Oceanic Eng.* **23**(4), 400–410 (1998).
- <sup>7</sup>T. G. Leighton, “Nonlinear bubble dynamics and the effects on propagation through near-surface bubble layers,” *AIP Conf. Proc.* **728**, 180–193 (2004).
- <sup>8</sup>T. G. Leighton, “From seas to surgeries, from babbling brooks to baby scans: The acoustics of gas bubbles in liquids,” *Int. J. Modern Phys. B* **18**(25), 3267–3314 (2004).
- <sup>9</sup>A. D. Phelps, D. G. Ramble, and T. G. Leighton, “The use of a combination frequency technique to measure the surf zone bubble population,” *J. Acoust. Soc. Am.* **101**(4), 1981–1989 (1997).
- <sup>10</sup><http://www.isvr.soton.ac.uk/fdag/TWIPS/index.htm> “Repository for TWIPS data,” (Last viewed February 24, 2010).
- <sup>11</sup>T. G. Leighton, D. C. Finfer, and P. R. White, “Bubble acoustics: What can we learn from cetaceans about contrast enhancement?,” *Proceedings of the IEEE International Ultrasonics Symposium*, Rotterdam, Netherlands, 18–21 September 2005, pp. 964–973 (2005).
- <sup>12</sup>T. G. Leighton, D. C. Finfer, P. R. White, G.-H. Chua, and J. K. Dix, “Wake penetrating sonar,” *Proceedings of EAA EUROREGIO 2010*, Ljubljana, Slovenia, Paper 163 (September 15–18, 2010), 8 pp.
- <sup>13</sup>T. G. Leighton, S. D. Meers, and P. R. White, “Propagation through nonlinear time-dependent bubble clouds and the estimation of bubble populations from measured acoustic characteristics,” *Proc. R. Soc. Lond. A* **460**(2049), 2521–2550 (2004).
- <sup>14</sup>J. S. Zhang, S. Y. Lin, P. Liu, R. C. Miao, and W. M. Yang, “Sound speed in bubble film of ship wakes,” *Sci. Chin. Ser. G* **51**(1), 64–71 (2008).
- <sup>15</sup>C. I. Malme, “Method of measuring the acoustic properties of ship wakes,” *J. Acoust. Soc. Am.* **58**(Suppl. 1), S102 (1975).
- <sup>16</sup>X. Di, “Predicting acoustic propagation through bubble ship wakes using a PE model,” ARL Technical Report 00-003 (2000), Applied Research Laboratory, The Pennsylvania State University, State College, PA.
- <sup>17</sup>B. R. Rapids and R. L. Culver, “An acoustic ship wake for propagation studies,” ARL Technical Memorandum 00-068 (2000), Applied Research Laboratory, The Pennsylvania State University, State College, PA.
- <sup>18</sup>G. O. Marmorino and C. L. Trump, “Preliminary side-scan ADCP measurements across a ship’s wake,” *J. Atmos. Oceanic Technol.* **13**, 507–513 (1996).
- <sup>19</sup>R. L. Culver and D. L. Bradley, “Measured turbulence in ship wakes,” *J. Acoust. Soc. Am.* **110**(5), 2642 (2001).
- <sup>20</sup>A. Sutin, A. Benilova, H. S. Roh, and Y. Nah, “Acoustic measurements of bubbles in the wake of ship models,” *Proceedings of the 3rd International Conference on Underwater Acoustic Measurements: Technologies and Results*, Napflion, Crete, pp. 767–772 (2009).

- <sup>21</sup>R. D. Peltzer, O. M. Griffin, W. R. Barger, and J. A. C. Kaiser, "High-resolution measurement of surface-active film redistribution in ship wakes," *J. Geophys. Res.* **97**(C4), 5231–5252 (1992).
- <sup>22</sup>A. Smirnov, I. Celik, and S. Shi, "LES of bubble dynamics in wake flows," *Comput. Fluids* **34**, 351–373 (2005).
- <sup>23</sup>H. Burch, S. Vagle, M. J. Buckingham, and D. M. Farmer, "Sound propagation through the near-surface bubble layer," *Proceedings of the 3rd European Conference on Underwater Acoustics*, Crete, pp. 1161–1166 (1996).
- <sup>24</sup>M. V. Trevorrow, S. Vagle, and D. M. Farmer, "Acoustical measurements of microbubbles within ship wakes," *J. Acoust. Soc. Am.* **95**(4), 1922–1930 (1994).
- <sup>25</sup>H. A. Dumbrell, "Comparison of excess attenuation and backscatter measurements of ship wakes," in *Natural Physical Processes Associated with Sea Surface Sound*, edited by T. G. Leighton (ISVR, University of Southampton, UK), pp. 171–178 (1997).
- <sup>26</sup>T. C. Gallaudet and C. P. de Moustier, "Multibeam echo-sounding measurement of the microbubble field in a ship's wake," *J. Acoust. Soc. Am.* **111**, 2345 (2002).
- <sup>27</sup>R. L. Culver and M. F. Trujillo, "Measuring and modeling bubbles in ship wakes, and their effect on acoustic propagation," *Proceedings of the 2nd International Conference on Underwater Acoustic Measurements: Technologies and results*, FORTH, Crete (June 25–29, 2007), pp. 563–570.
- <sup>28</sup>D. L. Bradley, R. L. Culver, X. Di, and L. Bjorno, "Acoustic qualities of ship wakes," *Proceedings of the 6th European Conference on Underwater Acoustics*, Gdansk, Poland (June 24–27, 2002).
- <sup>29</sup>R. L. Culver, T. C. Weber, and D. L. Bradley, "The use of multi-beam sonars to image bubbly ship wakes," *Proceedings of the International Conference Underwater Acoustic Measurements: Technologies & Results Heraklion*, Crete Greece, (June 28 to July 1, 2005), pp. 509–516.
- <sup>30</sup>S. Vagle and H. Burch, "Acoustic measurements of the sound-speed profile in the bubbly wake formed by a small motor boat," *J. Acoust. Soc. Am.* **117**(1), 153–163 (2005).
- <sup>31</sup>R. L. Culver and M. F. Trujillo, "Measuring and modeling bubbles in ship wakes, and their effect on acoustic propagation," *Proceedings of the 2nd International Conference on Underwater Acoustic Measurements: Technologies and Results*, Forth, Crete (2007), pp. 563–570.
- <sup>32</sup>National Defense Research Committee, "Role of bubbles in acoustic wakes," in *Physics of Sound in the Sea*, NAVMAT Rep. p-9675 (Peninsula Publishing, Los Altos, CA, 1945).
- <sup>33</sup>D. M. Farmer and D. D. Lemon, "The influence of bubbles on ambient noise in the ocean at high wind speeds," *J. Phys. Oceanogr.* **14**, 1762–1778 (1984).
- <sup>34</sup>T. G. Leighton and G. B. N. Robb, "Preliminary mapping of void fractions and sound speeds in gassy marine sediments from subbottom profiles," *J. Acoust. Soc. Am.* **124**(5), EL313–EL320 (2008).
- <sup>35</sup>T. G. Leighton, D. G. Ramble, A. D. Phelps, C. L. Morfey, and P. P. Harris, "Acoustic detection of gas bubbles in a pipe," *Acust. Acta Acust.* **84**(5), 801–814 (1998).
- <sup>36</sup>See supplemental material at E-JASMAN-130-010191 for movie files. Interested readers are also advised to see <http://www.isvr.soton.ac.uk/fdag/TWIPS/index.htm>, which contains additional material, and to see T. G. Leighton, D. C. Finfer, P. R. White, G-H. Chua, and J. K. Dix, "Clutter suppression and classification using twin inverted pulse sonar (TWIPS)," *Proc. R. Soc. London, Ser. A* **466**, 3453–3478 (2010). For more information see <http://www.aip.org/pubservs/epaps.html>.